

## A study of the structural phase transformation in the shape memory alloy $\text{Co}_2\text{NbSn}$

This article has been downloaded from IOPscience. Please scroll down to see the full text article.

2002 J. Phys.: Condens. Matter 14 1371

(<http://iopscience.iop.org/0953-8984/14/6/322>)

View [the table of contents for this issue](#), or go to the [journal homepage](#) for more

Download details:

IP Address: 171.66.16.27

The article was downloaded on 17/05/2010 at 06:09

Please note that [terms and conditions apply](#).

# A study of the structural phase transformation in the shape memory alloy $\text{Co}_2\text{NbSn}$

K-U Neumann<sup>1</sup>, T Kanomata<sup>1,2</sup>, B Ouladdiaf<sup>3</sup> and K R A Ziebeck<sup>1</sup>

<sup>1</sup> Department of Physics, Loughborough University, LE11 3TU, UK

<sup>2</sup> Faculty of Engineering, Tohoku Gakuin University, Tagajo 985-8537, Japan

<sup>3</sup> Institut Laue Langevin, BP156 Grenoble 38042, France

Received 24 October 2001

Published 1 February 2002

Online at [stacks.iop.org/JPhysCM/14/1371](http://stacks.iop.org/JPhysCM/14/1371)

## Abstract

Resistivity, specific heat and magnetization measurements on the shape memory compound  $\text{Co}_2\text{NbSn}$  corroborate the presence of ferromagnetic order below 119 K and a structural phase transition at 235 K. High-resolution neutron powder diffraction measurements confirmed that the high-temperature cubic phase has the Heusler  $L2_1$  structure and established that the low-temperature phase is orthorhombic with space group  $Pmma$ . The thermal variation of the specific heat at low temperatures indicates a high density of states consistent with electronic structure calculations and a band Jahn–Teller mechanism for the transformation.

## 1. Introduction

Recently Heusler alloys have gained renewed interest due to their potential for use as smart materials, for example, ferromagnetic shape memory alloys [1] or for developing spin-dependent electronics [2].  $\text{Ni}_2\text{MnGa}$  is the only known ferromagnetic material exhibiting a martensitic transition from a high-temperature Heusler structure to a related tetragonal form [3] with a 6.6%  $c$  axis contraction at  $T_M = 200$  K. Associated with this phase transition the material exhibits shape memory properties enabling the system to reverse large deformations in the martensitic phase by heating into the cubic phase. The interest in ferromagnetic shape memory compounds stems from the possibility of controlling the phase transition by application of a magnetic field [4]. The response of the system to a field is potentially faster than that obtained by changing temperature or applying stress, thus substantially increasing the range of applications. As a consequence the material has become one of the most actively researched shape memory alloys being the subject of more than half the papers presented at the recent ‘SMART 2000’ Conference in Sendai [1].

$\text{Co}_2\text{NbSn}$  is also reported to belong to the group of ferromagnetic shape memory Heusler alloys. However, unlike  $\text{Ni}_2\text{MnGa}$  [3], for which the martensitic phase transition ( $T_m = 200$  K) occurs within the ferromagnetically ordered phase ( $T_c = 376$  K), for  $\text{Co}_2\text{NbSn}$  the martensitic

phase transition temperature  $T_m = 235$  K [5] ( $T_m = 253$  K [6]) is well above the ferromagnetic ordering temperature of  $T_c = 119$  K [1]. Consequently the shape memory behaviour in  $\text{Co}_2\text{NbSn}$  cannot be controlled by a magnetic field. From x-ray diffraction measurements the low temperature transformed phase of  $\text{Co}_2\text{NbSn}$  has variously been reported as being tetragonal with  $a = 6.21$  Å and  $c = 6.06$  Å [6] or orthorhombic [5] with  $a = 8.87$  Å,  $b = 8.79$  Å,  $c = 5.94$  Å. However, in the latter study the  $c$ -axis was reported to be non-orthogonal with  $\gamma = 89.50^\circ$ . On the basis of magnetisation measurements the magnetic moment per Co atom at 0 K was estimated to be  $0.36 \mu_B$  [7]. On alloying, e.g.  $(\text{Co}_{1-x}\text{Ni}_x)_2\text{NbSn}$ , or with the application of pressure [8] the Co moment diminishes with ferromagnetic order and the martensitic phase transition disappearing at the same critical concentration for alloying or pressure. This points to an intricate relationship between the occurrence of ferromagnetic order and the lattice instability in  $\text{Co}_2\text{NbSn}$ . As with other isostructural compounds the electron concentration and hence band filling plays an essential role influencing both the structural instability and the occurrence of a ferromagnetic ground state. Between the Curie temperature and  $\sim 220$  K the inverse magnetic susceptibility has an approximately linear dependence on temperature yielding an effective paramagnetic moment per cobalt atom of  $1.2 \mu_B$ . Above  $T_m$  the variation is again essentially linear but characterized by a larger effective moment of  $1.83 \mu_B$  per Co atom [4]. This observation would suggest that the compound falls into the class of weak itinerant ferromagnets. On the basis of band structure calculations it was argued that it is a common mechanism that drives the phase transition in both  $\text{Ni}_2\text{MnGa}$  and  $\text{Co}_2\text{NbSn}$ , namely the band Jahn–Teller effect [8] which was originally proposed to account for the structural transition observed in A15 compounds [9]. In this model, the lattice distortion breaks the degeneracy of the bands in the vicinity of the Fermi level, thus causing a redistribution of electrons in these bands with a consequent reduction of the free energy. Thus it is important to establish the structure of the low-temperature phase as a basis for understanding the mechanism giving rise to the phase transition and ultimately the shape memory effect. Therefore a high resolution powder neutron diffraction study has been carried out in the ferromagnetic transformed phase and the cubic high temperature paramagnetic phase. Since the magnetic and structural properties in these compounds depend sensitively on the degree of atomic order, resistivity, specific heat and magnetisation measurements were also carried out and compared with earlier studies.

## 2. Experimental

A 20 g sample of  $\text{Co}_2\text{NbSn}$  was prepared by the repeated melting of the appropriate quantities of constituent elements of 4 N purity in an argon arc furnace. Specimens suitable for specific heat, resistivity and magnetization measurements were spark eroded from the resultant ingot with the remainder being crushed in a hardened steel pestle and mortar to a particle size of  $<250 \mu\text{m}$ . The powder and solid pieces were then sealed under a reduced argon atmosphere in a quartz ampoule and annealed at  $800^\circ\text{C}$  for 48 h after which it was quenched into cold water. Subsequent x-ray powder diffraction measurements at room temperature confirmed the sample to be of single phase with the Heusler  $L2_1$  structure (space group  $Fm\bar{3}m$ ) and lattice parameter of  $6.143$  Å. Further x-ray measurements at low temperatures showed that the specimen had a structural phase transition at  $235 \pm 5$  K.

Resistivity measurements were carried out using the four terminal technique with the sample in thermal contact with the second stage of a closed cycle refrigerator. Although the magnetic properties of  $\text{Co}_2\text{NbSn}$  have previously been reported [6, 7] further measurements were carried out to characterise the specimen. The measurements were made using a SQUID magnetometer in accurately controlled fields up to 5 T and at temperatures between 2 and 300 K. Demagnetising corrections were applied to the values of the externally applied field.

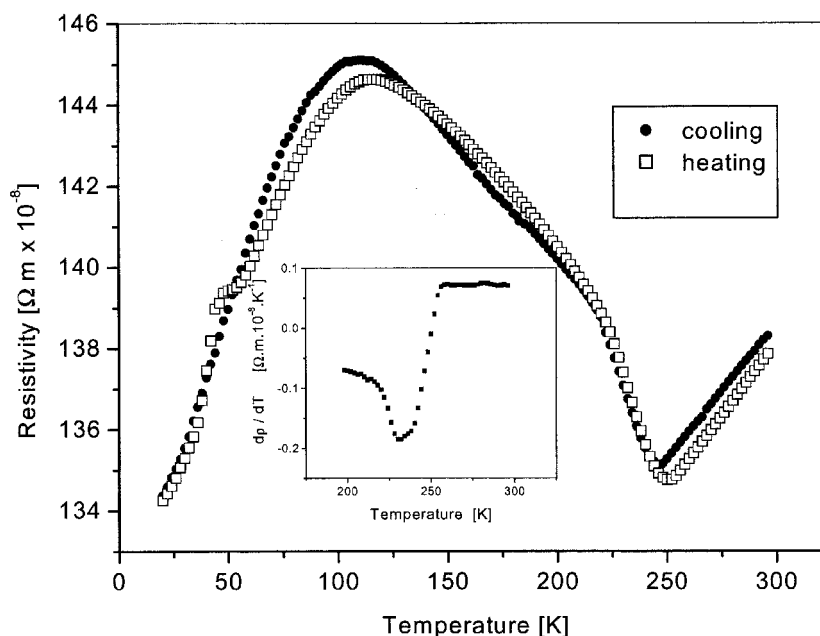


**Figure 1.** The thermal variation of the resistivity measured whilst heating and cooling between 15 and 300 K. The inset shows the derivative of the resistivity in the vicinity of the structural phase transition for the heating cycle.

A quantitative investigation of the crystallographic structure in both the high- and low-temperature phases was undertaken using the high-resolution neutron powder diffractometer D1A at the ILL in Grenoble. For these measurements the specimen was contained in a thin walled vanadium can located in an 'orange' helium flow cryostat on the omega table of the diffractometer. Data were collected over the two theta range  $10^\circ$ – $160^\circ$  in steps of  $0.05^\circ$  using a wavelength of  $1.911 \text{ \AA}$

### 2.1. Results

The resistivity results obtained in cooling from room temperature to 15 K and then warming again to room temperature are shown in figure 1. From this figure it may be seen that the results exhibit a degree of hysteresis. A maximum in the resistivity, for both heating and cooling is observed in the vicinity of 100 K which is consistent with the reported value of the Curie temperature. At higher temperatures the resistivity passes through a relatively sharp minimum around 248 K, a value which is intermediate of those reported for the structural phase transition. Close examination of the thermal variation of the resistivity shows a pronounced change in slope at approximately 220 K. A more precise value of the transition temperature  $T_m$  was obtained by differentiating the data with respect to temperature. The resulting variation for the cooling cycle is shown as the insert to figure 1. As may be seen, the analysis produced a well defined minimum at  $228 \pm 6$  and  $233 \pm 6$  K for the cooling and heating cycle respectively. Above  $\sim 250$  K the resistivity increases approximately linearly with temperature.

Initially the magnetization was determined in a field of 0.1 T over the temperature range 5–300 K. These results indicated transitions in the vicinity of 115 and 220 K in agreement with the reported magnetic and structural phase transitions. From figure 2 it may be seen that in the ferromagnetic phase there is a point of inflection in the magnetization around 26 K. This arises

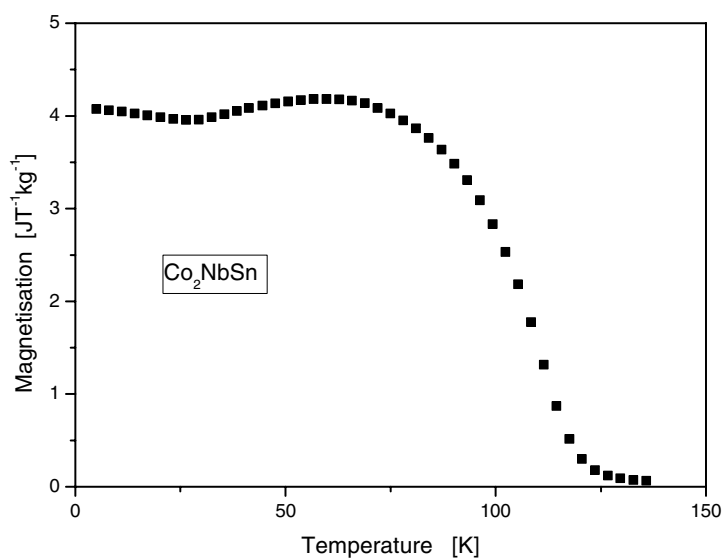


**Figure 2.** The magnetisation of  $\text{Co}_2\text{NbSn}$  measured in a field of 0.1 T for temperatures up to 130 K.

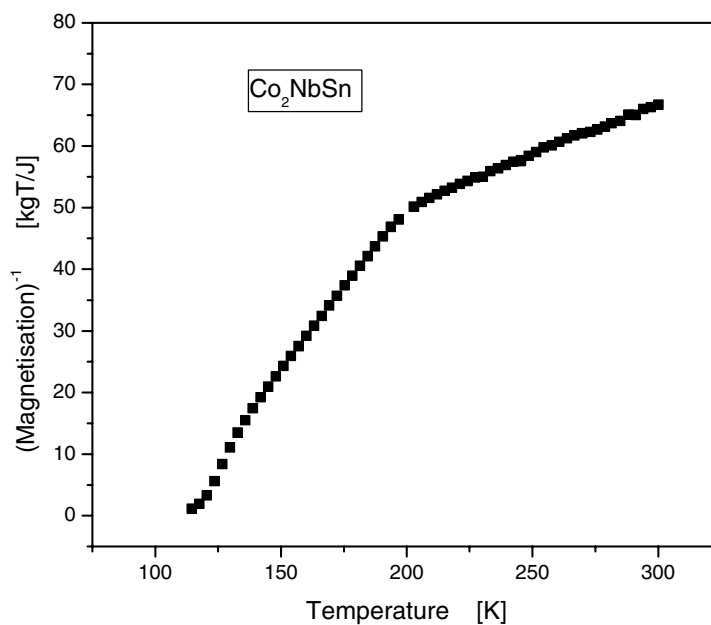


**Figure 3.** The inverse magnetisation of  $\text{Co}_2\text{NbSn}$  measured in a field of 0.1 T for temperatures between 110 and 300 K.

from the influence of magnetic anisotropy and applied magnetic field on the magnetization. In the paramagnetic regime the magnetization in a field of 0.1 T has essentially a Curie Weiss variation. Up to  $\sim 200$  K the inverse magnetization, as shown in figure 3, increases linearly with temperature characterised by a gradient of  $0.567 \text{ kg T J}^{-1}$  and extrapolated intercept temperature of 110 K. Above  $\sim 230$  K the variation is again linear but with a smaller gradient of  $0.172 \text{ kg T J}^{-1}$  and negative extrapolated intercept of 91 K. The result is consistent with the

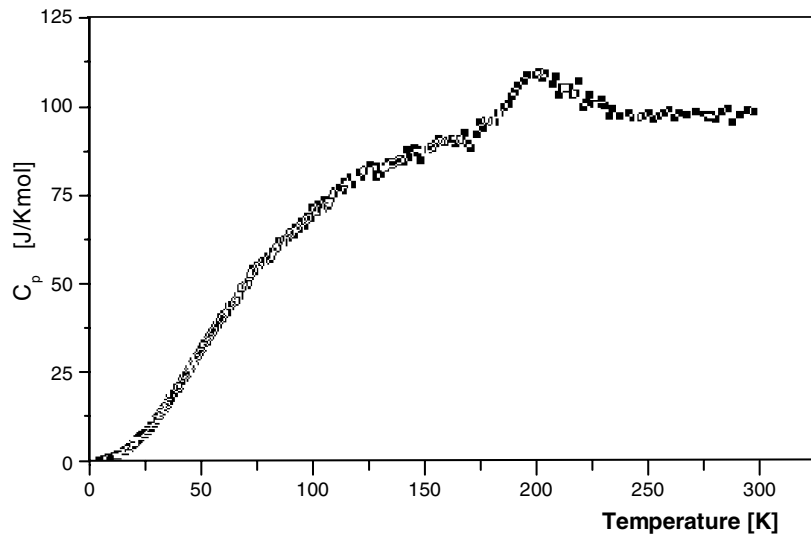


Figure 4. The specific heat of Co<sub>2</sub>NbSn as a function of temperature between 5 and 300 K.

change in structural symmetry and the introduction of anisotropy in the transformed phase. The two lines intersect at 200 K, a temperature significantly lower than the value for  $T_m$  indicated by the resistivity measurements. Based on the preliminary magnetization measurement a series of isotherms at 5° intervals were determined from which Arrott plots were produced. However only in the vicinity of the Curie temperature were the Arrott plots linear. The spontaneous magnetization and the inverse susceptibility were obtained by extrapolating the high field portion of the isotherms. Using the data obtained above 230 K, a Curie Weiss analysis was undertaken, the results of which are given in table 1. In this table the paramagnetic moment  $\mu_p$  was obtained from the effective moment  $p_{\text{eff}}$  using  $p_{\text{eff}}^2 = \mu_p(\mu_p + 2)$ .

The specific heat  $C_p$ , of Co<sub>2</sub>NbSn, as a function of temperature between 5 and 300 K is shown in figure 4. A broad anomaly is observed between 180 and 240 K with a maximum at 200 K. This temperature range covers the region where anomalies were observed in the x-ray, resistivity and magnetization measurements consistent with the change in crystal structure. Martensitic phase transitions often give rise to an anomaly in the specific heat of finite width as a result of the system not being in thermal equilibrium. Owing to the small magnetic moment an anomaly at the Curie temperature was not observed. In order to compare the low-temperature variation of the specific heat with earlier measurements [10], the same functional form was used to analyse the data. Since the moment per cobalt atom is small only the electronic and phonon contributions were considered

$$C_p = \gamma T + \beta T^3.$$

The term linear in  $T$  gives the electronic Sommerfeld coefficient  $\gamma$  and the second term is attributed to lattice vibrations. The Debye approximation is valid for temperatures below  $\sim \Theta_D/12$  where  $\Theta_D$  is the Debye temperature given by

$$\Theta_D = \sqrt[3]{\frac{234 R}{\beta}}.$$

The results of a linear regression which are given in table 1 are in good agreement with those reported by Brandão *et al* [10].

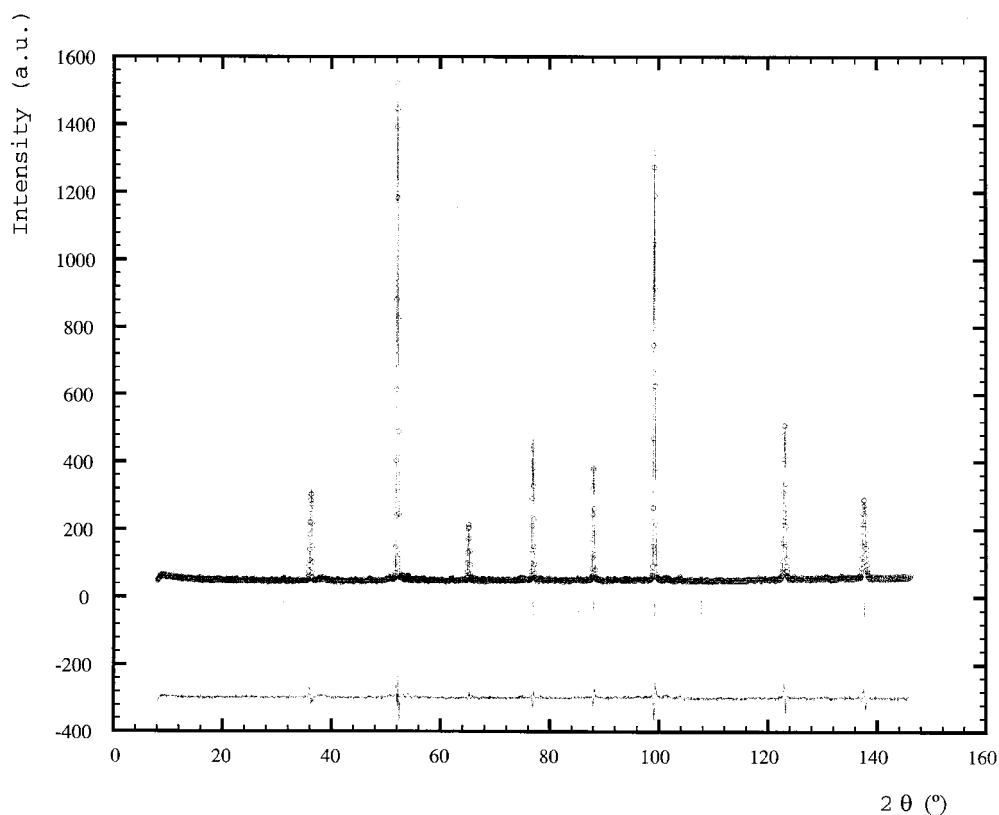


**Figure 5.** The observed and calculated neutron powder diffraction patterns of  $\text{Co}_2\text{NbSn}$  at 275 K together with the difference pattern.

**Table 1.** The results of magnetic and heat capacity measurements on  $\text{Co}_2\text{NbSn}$ . The value of moment given in the first column was obtained in a field of 5 T at 5 K and the paramagnetic results were obtained from Arrott plots in the cubic phase.

| $\mu_{5,5}$ ( $\mu_B$ ) | $T_c$ (K)   | $p_{\text{eff}}/\text{Co}$ ( $\mu_B$ ) | $\mu_p$ ( $\mu_B$ ) | $\Theta_p$ (K) | $\gamma$ ( $\text{mJ K}^{-2} \text{mol}^{-1}$ ) | $\beta$ ( $\text{mJ K}^{-4} \text{mol}^{-1}$ ) | $\Theta_D$ (K) |
|-------------------------|-------------|--|---------------------|----------------|---|--|----------------|
| $0.38 \pm 0.01$         | $115 \pm 5$ | $1.69 \pm 0.01$                        | $0.97 \pm 0.01$     | $35 \pm 2$     | $22 \pm 2$                                      | $0.49 \pm 0.006$                               | $251 \pm 2$    |

## 2.2. Neutron diffraction

The Bragg peaks observed at 275 K could be indexed on a face centred cubic lattice consistent with the sample being of single phase. A profile refinement confirmed that the specimen was highly ordered in the Heusler  $L2_1$  structure. Details of the structural parameters obtained from the refinement are given in the first column of table 2 and the observed and calculated diffraction patterns are shown in figure 5 together with the difference pattern. A statistical chi-squared test was applied to the fit, defined by

$$\chi^2 = \sum \frac{(F_{\text{obs}} - F_{\text{calc}})^2}{(\sigma F_{\text{obs}})^2} / (N_{\text{obs}} - N_{\text{par}}).$$

( $N_{\text{obs}}$  is the number of observations and  $N_{\text{par}}$  is the number of parameters.)

**Table 2.** Crystallographic parameters of Co<sub>2</sub>NbSn obtained from the profile refinement.

| $T = 275$ K                                    | $T = 50$ K  |
|--|---|
| Cubic Heusler L2 <sub>1</sub> ( $Fm\bar{3}m$ ) | Orthorhombic ( $Pmma$ )   |
| Nb (4a) 0 0 0                                  | Co (4h) $0 y \frac{1}{2}$ ; $y = 0.24899(11)$                   |
| Sn (4b) $\frac{1}{2} \frac{1}{2} \frac{1}{2}$  | Co (4k) $\frac{1}{4} y z$ ; $y = 0.7572(2)$ ; $z = 0.05938(51)$ |
| Co (8c) $\frac{1}{4} \frac{1}{4} \frac{1}{4}$  | Nb (2a) 0 0 0   |
|  | Nb (2f) $\frac{1}{4} \frac{1}{2} z$ ; $z = 0.52585(31)$         |
|  | Sn (2e) $\frac{1}{4} 0 z$ ; $z = 0.54109(41)$                   |
|  | Sn (2b) $0 \frac{1}{2} 0$                                       |
| $a = 6.1465(2)$ Å                              | $a = 8.7874(2)$ Å   |
|  | $b = 5.9472(2)$ Å   |
|  | $c = 4.4278(2)$ Å   |
| Volume = $232.211(1)$ Å <sup>3</sup>           | Volume = $231.398(1)$ Å <sup>3</sup>                            |
| $\chi^2 = 6.3$                                 | $\chi^2 = 3.75$   |

On cooling to 50 K the diffraction pattern became considerably more complicated. Some of the original cubic peaks split and additional peaks appeared. The splitting of the Bragg reflections is consistent with the loss of cubic symmetry while the appearance of new peaks suggests that the translational symmetry is altered. The list of non-cubic, non-isomorphic subgroups of the space group  $Fm\bar{3}m$  includes the tetragonal space group  $Imma$  which is appropriate for the distorted phase of the related compound Ni<sub>2</sub>MnGa. However, it is apparent from the number of reflections and their relative intensities that the low temperature phase is not tetragonal. Close inspection of the peaks and in particular those formally of the form  $(h + k + l) = 2n$  or  $4n$  suggest that they split into three. An initial refinement was carried out using an orthorhombic structure with lattice parameters  $a = 4.4237$  Å,  $b = 4.3892$  Å,  $c = 5.9417$  Å and space group  $Imma$ , as proposed by [5]. This structure accounted for the splitting of the intense peaks but was unable to account for the additional weak ones. The position of the weak peaks could be accounted for by doubling the length of the  $a$  axis. However, in order to have intensity at these positions it was necessary to reduce the symmetry to  $Pmma$ . Transposing the axes  $z' \rightarrow y \rightarrow x \rightarrow z$  such that the setting of the unit cell is consistent with that defined in the International tables (#51), the atomic positions are as given in table 2. From this table it may be seen that only one Nb and one Sn atom occupy special positions. An initial refinement was performed using these parameters and the space group  $Pmma$ . This structure accounted for all the observed peaks and did not generate any additional ones. The refinement was repeated, this time allowing the positional parameters of those atoms in general positions to vary. This led to significant improvement. The parameters obtained from the refinement are shown in the second column of table 2 and the observed and calculated diffraction patterns together with the difference pattern in figure 6.

### 3. Discussion

The lattice parameters obtained in the structural refinement show that the volume of the unit cell in the high- and low-temperature structures is similar, i.e. <0.3% difference. In Co<sub>2</sub>NbSn the transition takes place in the paramagnetic phase. This is in contrast to Ni<sub>2</sub>MnGa in which there is a 3% change in cell volume between the low- and high-temperature phases. It is of interest to compare these results with those obtained on other systems undergoing structural phase



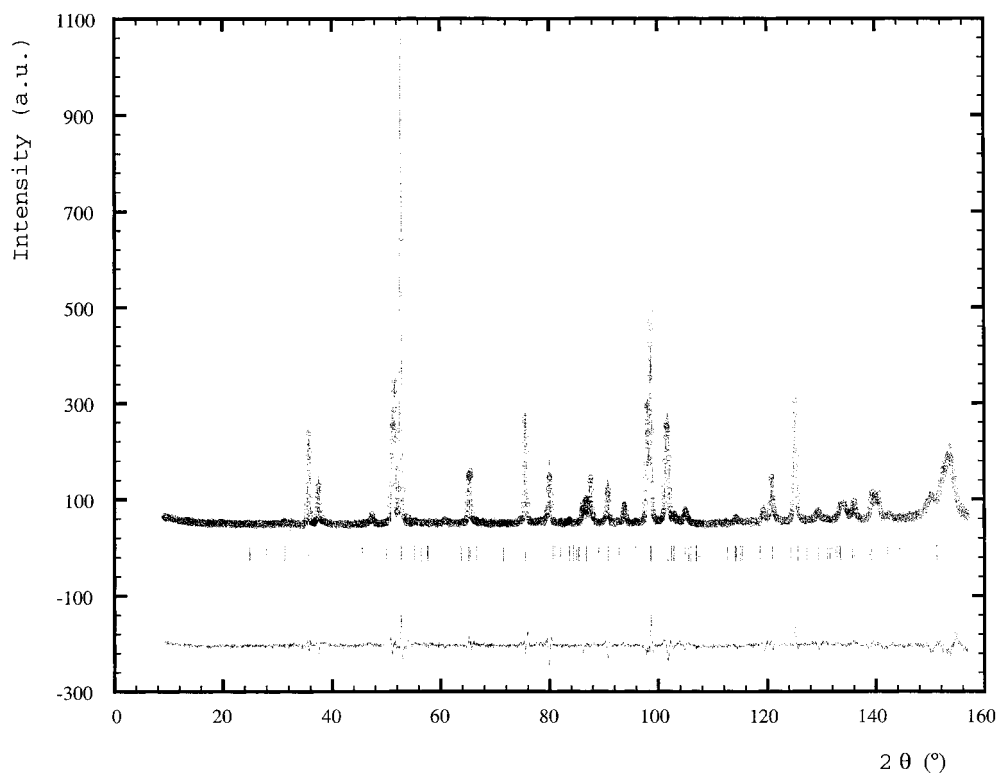


**Figure 6.** The observed and calculated neutron powder diffraction patterns of  $\text{Co}_2\text{NbSn}$  at 50 K together with the difference pattern.

transitions. A significant change in the crystal structure is observed at the metal–insulator transition of  $\text{V}_2\text{O}_3$  involving  $\sim 3.5\%$  reduction in cell volume [11] and loss of long-range antiferromagnetic order in the metallic phase. The loss of long-range magnetic order at the structural phase transition is not dissimilar to the behaviour found in  $\text{YMn}_2$  [12] where a paramagnetic state is established at a first-order phase transition involving a  $\sim 5\%$  reduction in cell volume. This behaviour is associated with a collapse of the local Mn moment. However the strong thermal variation of the susceptibility above the Curie temperature in  $\text{Co}_2\text{NbSn}$  in both the transformed and cubic phases indicates that a significant magnetic response persists. Analysis of the data shown in figure 3 yields a paramagnetic moment  $\mu_p$  in both regions which is larger than the ground state value. This is confirmed by the results obtained from the Arrott plots in the cubic phase and shown in table 1. A large paramagnetic moment can arise from spin fluctuations in which the long wavelength components are enhanced. This is quite possible in  $\text{Co}_2\text{NbSn}$  since the cobalt atoms carrying the moment are separated by  $a/2$  and hence there is significant overlap of the  $d$  functions. In those Heusler alloys in which the moment is confined to the Mn atoms there is negligible overlap of the  $d$  functions and hence the magnetic properties are characteristic of local moments of fixed amplitude. In the paramagnetic phase the moments become spatially disordered but  $\mu_p$  has the same value as  $\mu_0$  in the ground state. Measurements at 4.2 K and in fields of up to 20 T show that the magnetization of  $\text{Co}_2\text{NbSn}$  does not saturate [5] as expected for weak itinerant ferromagnetism. However, the increase in moment with field is small  $\sim 16\%$  in 20 T, remaining significantly

smaller than  $\mu_p$ . In fact the magnetic properties of Co<sub>2</sub>YZ compounds fall into two groups [13]. Those compounds containing group 4A and 4B elements or 5A and 3B elements have relatively large magnetic moments and Curie temperatures with the paramagnetic moment  $\mu_p$  being close to the ground state value. Compounds containing group 4A and 3B elements or group 5A and 4B elements have smaller magnetic moments and lower Curie temperatures but have paramagnetic moments larger than the ground state values.

The increase in resistivity between the structural phase transition and Curie temperature is indicative of semi-conductor behaviour. However, whether this property arises from conventional band structure effects, i.e. a gap opens up at  $T_m$  or from many body effects, for example electron–electron or electron–phonon correlations cannot be decided on the basis of the present measurements alone. The variation of the magnetization with temperature would suggest a many-body mechanism. Spectroscopy measurements are required to clarify this observation. The value obtained for the Sommerfeld coefficient  $\gamma = 22 \text{ mJ K}^{-2} \text{ mol}^{-1}$  is significantly larger than that expected for a normal metal suggesting a large density of states at the Fermi level. For non interacting electrons the Sommerfeld coefficient  $\gamma(0)$  is proportional to the bare electronic density of states and therefore  $n(\epsilon_F) = 0.212\gamma$  which yields 4.7 (states/(eV atom)). This result is consistent with the band structure calculations of Fujii *et al* [8]. The calculations which were undertaken using both the LMTO and KKR methods and for cubic and tetragonal forms of Co<sub>2</sub>NbSn yield a peak in the density of states at the Fermi level. The peak is predicted to come primarily from the d bands of cobalt and niobium, which give rise to 2.9 and 1.1 states/atom eV respectively. On the basis of these calculations it was argued that it is the redistribution of electrons around the Fermi level which drives the structural phase transition [8]. The reduction in symmetry is able to lift the degeneracy of electronic bands at the Fermi level causing the peak in the density of states to split. Combined with the energy required for creating the lattice distortion the resulting shift in the energy of bands and the resulting re-population of these bands lowers the free energy of the whole system making such a transformation energetically favourable. A polarised neutron diffraction measurement of the unpaired spin distribution in the related shape memory compound Ni<sub>2</sub>MnGa has revealed a change in symmetry at the phase transition [14]. On the basis of this measurement it was proposed that the phase transition was driven by a band Jahn–Teller mechanism. The present results suggest that the same mechanism is responsible for the phase transition in Co<sub>2</sub>NbSn.

#### 4. Conclusion

Neutron diffraction measurements have enabled the low-temperature structure to be determined and the previous ambiguity based on limited x-ray measurements to be resolved. Analysis of the low-temperature specific heat indicates a high density of states at the Fermi surface in agreement with band structure calculations. The analysis supports the contention that the phase transition in Co<sub>2</sub>NbSn is driven by a redistribution of electrons which occurs in the band Jahn–Teller mechanism observed in the related compound Ni<sub>2</sub>MnGa. The magnetic properties of the cobalt compound are, however, characteristic of weak itinerant ferromagnetism in which the paramagnetic state is characterized by spin fluctuations.

#### References

- [1] *Proc. SMART-2000 (Sendai, Japan)*
- [2] Yu Irkhin V and Katsnel'son M I 1994 *Phys.–Usp.* **37** 659
- [3] Webster P J, Ziebeck K R A, Town S L and Peak M S 1984 *Phil. Mag.* **B 49** 295

- [4] Ma Y, Awaji S, Watanabe M, Matsumoto M and Kobayashi N 2000 *Solid State Commun.* **113** 671
- [5] Kanomata T 2001 unpublished
- [6] Terada M, Fujita Y and Endo K 1974 *J. Phys. Soc. Japan* **36** 620
- [7] Ziebeck K R A and Webster P J 1974 *J. Phys. Chem. Solids* **35** 1
- [8] Fujii S, Ishida S and Asano S 1989 *J. Phys. Soc. Japan* **58** 3657
- [9] Labbé J and Friedel J 1966 *J. Phys. Radium* **27** 153 and 303
- [10] Brandão D E, Boff M A, Fraga G L F and Grandi T A 1993 *Phys. Status Solidi* **176** K45
- [11] Yethiraj M J 1990 *Solid State Chem.* **88** 53
- [12] Nakamura Y, Shiga M and Kawano S 1983 *Physica B* **120** 212
- [13] Webster P J and Ziebeck K R A 1988 *Landolt Börnstein New Series 19c* ed H P J Wijn (Berlin: Springer)
- [14] Brown P J, Bargawi A Y, Crangle J, Neumann K-U and Ziebeck K R A 1999 *J. Phys.: Condens. Matter* **11** 4715